PCCP

Understanding Physical Chemistry of BaxSr1-xTiO3 using ReaxFF Molecular Dynamics Simulations

Journal:	*Physical Chemistry Chemical Physics*
Manuscript ID	CP-ART-07-2021-003353.R1
Article Type:	Paper
Date Submitted by the Author:	04-Sep-2021
Complete List of Authors:	Akbarian, Dooman; Pennsylvania State University, Mechanical Engineering Nayir, Nadire; Pennsylvania State University, Mechanical Engineering van Duin, Adri; The Pennsylvania State University, Mechanical Engineering

Understanding Physical Chemistry of $Ba_xSr_{1-x}TiO_3$ using ReaxFF Molecular Dynamics Simulations

Dooman Akbarian[1], Nadire Nayir[1,2,3] and Adri C. T. van Duin[1,2]*

[1] Department of Mechanical Engineering, Pennsylvania State University, University Park, Pennsylvania 16802, United States.

[2] 2-Dimensional Crystal Consortium (2DCC) Materials Research Institute, The Pennsylvania State University, University Park, Pennsylvania 16802, United States.

[3] Department of Physics, Karamanoglu Mehmetbey University, Karaman 70000, Turkey.

Corresponding Author. E-mail address: acv13@psu.edu

Abstract

Barium strontium titanate $Ba_xSr_{1-x}TiO_3$ (BSTO) has been widely used in nano devices due to its unique ferroelectric properties and can be epitaxially grown on $SrTiO_3$ (STO) support, with a reduced lattice and thermal mismatch. In this work, we developed a ReaxFF reactive force field verified against quantum mechanical data to investigate the temperature and composition dependency of BSTO in non-ferroelectric/ferroelectric phases. This potential was also explicitly designed to capture the surface energetics of STO with SrO and TiO_2 terminations. Our molecular dynamics simulations indicate that when the percentage of Sr increases, the phase transition temperature and the polarizations of the $Ba_xSr_{1-x}TiO_3$ system decrease monotonically. In addition, as the oxygen vacancy concentration enhances, the initial polarization and the phase transition temperature of the system drop significantly. Furthermore, our simulation results show that charge screening induced by adsorption of water molecules on TiO_2 terminated surfaces leads to an increased initial polarization.

Introduction

Barium strontium titanite $Ba_xSr_{1-x}TiO_3$ (BSTO) is a special class of ferroelectric perovskites with favorable physical properties such as low dielectric loss, high dielectric constant, and highly nonlinear dielectric response. Additionally, BSTO has exceptionally tunable ferroelectric properties due to dependency of structural phase transitions on composition x and temperature[1-3]. For instance, the phase transition temperature of BSTO elevates from 126 K to 391 K as x increases from 0.12 ($Ba_{0.12}Sr_{0.88}TiO_3$) to 1 ($BaTiO_3$)[4]. Due to these unique combinations of physical properties, BTSO has demonstrated a great potential for applications in capacitors for dynamic RAMs, tunable microwave devices, piezoelectric actuators, microsensors and varicap diodes[1-2, 5]. However, the aforementioned applications require a single crystalline BSTO whose physicochemical properties strongly depends on the substrate it is grown on. $SrTiO_3$ (STO) comes forth as a suitable substrate, which mitigates the lattice and thermal mismatch between the epilayer and substrate[6]. Additionally, STO has been effectively deployed in the epitaxial growth of thin film such as transition metal dichalcogenides, GaN, InP, Bi_2Se_3[7-9].

In order to formulate the design and optimization of next-generation materials for the aforementioned applications, it is necessarily to obtain atomistic-scale insight of the ferroelectric dynamics for the entire composition range of BSTO. Quantum mechanical (QM) methods such as density functional theory (DFT) were utilized to provide preliminary atomistic-scale understanding of the ferroelectric perovskites. However due to high computational costs, DFT-based dynamics methods are only possible for short time (~100 ps) and small length scales (~5 nm)[10]. Empirical force fields can be employed in molecular dynamics (MD) simulations to describe the ferroelectric perovskites at sufficiently large time and length scales. Previously-developed methods to investigate the physical properties of BSTO include the shell potential and

bond-valence force field[11-12]. In the shell potential, the valence electrons are modeled as a massless charged shell connected to a massive charged core. This potential has been utilized in several MD studies to analyze local structure and polarization, describe temperature versus composition phase diagram, and identify local-structure characteristics of the solid solutions[11, 13]. The bond-valence (BV) potential, which includes a bond-valence energy term measuring the unit cell asymmetry, was developed by Rappe et al. for ferroelectric perovskites [14]. This potential has since been parametrized for multiple ferroelectric materials such as BSTO to study the temperature and composition dependency of lattice constants and polarization[12]. Shell and BV potentials can be employed within a single BSTO formulation; however, they cannot be extended to study the interaction of BSTO structures in multi-material interfaces, and cannot describe chemical reactions.

To overcome this limitation of currently available BSTO potentials, we report here on the development and application of a ReaxFF BSTO description. The ReaxFF reactive force field is a bond-order based potential capable of simulating chemical reactions for a vast range of systems such as polymers, covalent and metal oxide/hydride/carbide materials and recently $BaTiO_3$ (BTO)[15-17]. In ReaxFF, bond orders are calculated from interatomic distances at every MD time step, allowing bond breakage and formation during the simulation[15]. Moreover, in ReaxFF polarization effects are computed using a geometry-dependent charge calculation scheme based on the electronegativity equalization method (EEM) and nonbonded interactions such as Coulomb and van der Waals and Coulomb interactions are calculated between every pair of atoms, regardless of their connectivity[15, 18]. In this study, we developed a $Ba_xSr_{1-x}TiO_3$ ReaxFF force field verified against DFT data. We subsequently employed this force field in MD simulations to investigate the impact of Sr/Ba composition ratio and oxygen vacancies (OV)

concentration on phase transition and polarization. Furthermore, we studied the effects of surface interactions with water on the polarization of the material.

Method

We used our recently developed BTO ReaxFF force field[17] as a starting point for the force field development. ReaxFF uses the following equation to describe the total energy of the system:[15]

$$E_{system} = E_{bond} + E_{over} + E_{under} + E_{lp} + E_{val} + E_{tor} + E_{vdWaals} + E_{coulomb} \quad (1)$$

where E_{bond} is the bond energy, E_{over} is an over-coordination penalty, E_{under} is an under-coordination stabilization, E_{lp} is the lone pair energy, E_{val} is the valence angle energy, E_{tor} is the torsion angle energy, $E_{vdWaals}$ is the nonbonded van der Waals energy and $E_{coulomb}$ is the nonbonded Coulombic energy.[15] A shielding term is employed in both the van der Waals and coulombic energy terms to avoid extra non-bonded interactions, and a Taper function is utilized to avoid discontinuity in these nonbonded energy terms[15].

The BSTO ReaxFF force field was developed by training against a set of DFT data including formation energies of different polymorphs of $SrTiO_3$ (STO) and BSTO alloy structures, OV in a tetragonal unit cell of STO, the volume/energy equations of state for the tetragonal and cubic STO and cubic BSTO phases, and the surface energies of stoichiometric and non-stoichiometric STO surfaces with TiO_2 and SrO surface terminations. In addition, the *Ba* and *Ti* metal data, BaO and TiO_2 oxide data[19-20] and BTO perovskite data[17] were included in the training set.

DFT calculations on periodic systems of STO and BSTO were performed using the Vienna *ab initio* Simulation Package (VASP)[21] with the projector augmented waves (PAW) method[22-23]. The effects of the exchange correlation energy functional were treated using the GGA-level Perdew−Burke− Ernzerhof scheme revised for solids (GGA-PBEsol).[24] Brillouin-zone

integration was sampled with a Γ-centered Monkhorst−Pack grid. In all structural calculations, atomic coordinates were relaxed with a plane-wave energy cutoff of 500 eV until the residual force on each atom is smaller than 0.01 eV/Å.

Surface energy, $E_{surface}$, for both stoichiometric and non-stoichiometric terminations is generally considered as a sum of cleavage, $E_{cleavage}$ which is an energy required for exfoliating slabs from their bulk form, and relaxation energies, $E_{relaxation}$ of a slab as shown in Equation 2[25-26].

$$E_{\text{surface}} = (E_{\text{cleavage}} + E_{\text{relaxation}})/A \qquad (2)$$

where A is the surface area. For stoichiometric surfaces with the stoichiometry of 1:1:3 for Sr:Ti:O, the cleavage and relaxation energies of each slab are computed using the equations of $E_{cleavage} = (E_{unrelaxed} - nE_{bulk})/2$ and $E_{relaxation} = (E_{total} - E_{unrelaxed})/2$.

For TiO_2 and SrO terminated nonstoichiometric surfaces with the stoichiometries of 2:3:8 and 3:2:7, the cleavage energy is computed by the following equation:

$$E_{\text{cleavage}}(\text{TiO}_2 + \text{SrO}) = (E_{\text{unrelaxed} - \text{TiO}_2} + E_{\text{unrelaxed} - \text{SrO} - \text{nEbulk}})/4A \qquad (3)$$

where $E_{unrelaxed\text{-}TiO2}+E_{unrelaxed\text{-}SrO}$ are the total energies of two unrelaxed complementary nonstoichiometric slabs, E_{bulk} is the bulk energy per formula unit in a cubic unit cell, n is the total number of bulk formula units in two slabs and 1/4 refers to four surfaces created upon the crystal cleavage. The relaxation energy of each slab is calculated by:

$$E_{\text{relaxation}} = {}^{1}/_{2}A(E_{\text{total}} - E_{\text{unrelaxed}}) \qquad (4)$$

E_{total} is the total energy of TiO_2 and SrO-terminated slabs after relaxation and 1/2 refers to two surfaces created upon the crystal cleavage.

Once the ReaxFF force field was developed, *NPT-MD* simulations were carried out on an 8 × 8 × 8 fully periodic BSTO supercell to derive the phase diagram dependency of BSTO on composition and vacancies. All systems were first energy minimized, then heated up and cooled down subsequently for 250 *ps* (time step 0.25 *fs*) using linear temperature regime *dT/dt* = 0.0012 *K/fs*. Berendsen barostat and thermostat were chosen with relatively weak coupling (barostat coupling: 2500 *fs* ; thermostat coupling: 100 *fs*). The unit cell polarization $P_u(t)$ was defined as:

$$P_u(t) = \frac{1}{V_u}\left(Z_{Ti}^{*} r_{Ti}(t) + \frac{1}{8} Z_X^{*} \sum_{i=1}^{8} r_{X,i}(t) + \frac{1}{2} Z_O^{*} \sum_{i=1}^{6} r_{O,i}(t)\right) \qquad (5)$$

where V_u is the unit cell volume, Z^* is the charge obtained using EEM, $r(t)$ is the atomic position in each unit cell at time t and X represents either Ba or Sr atoms. A Python script was developed to compute the unit cell polarizations across the supercell based on the atomic charges and positions provided by ReaxFF.

Results and Discussion

Figure 1 compares the DFT and ReaxFF values for heat of formation, stoichiometric/non-stoichiometric surface energies, and equations of state for STO in Pm3m and I4mcm phases and BSTO in cubic phase, indicating that ReaxFF results are in good agreement with the computed DFT values.

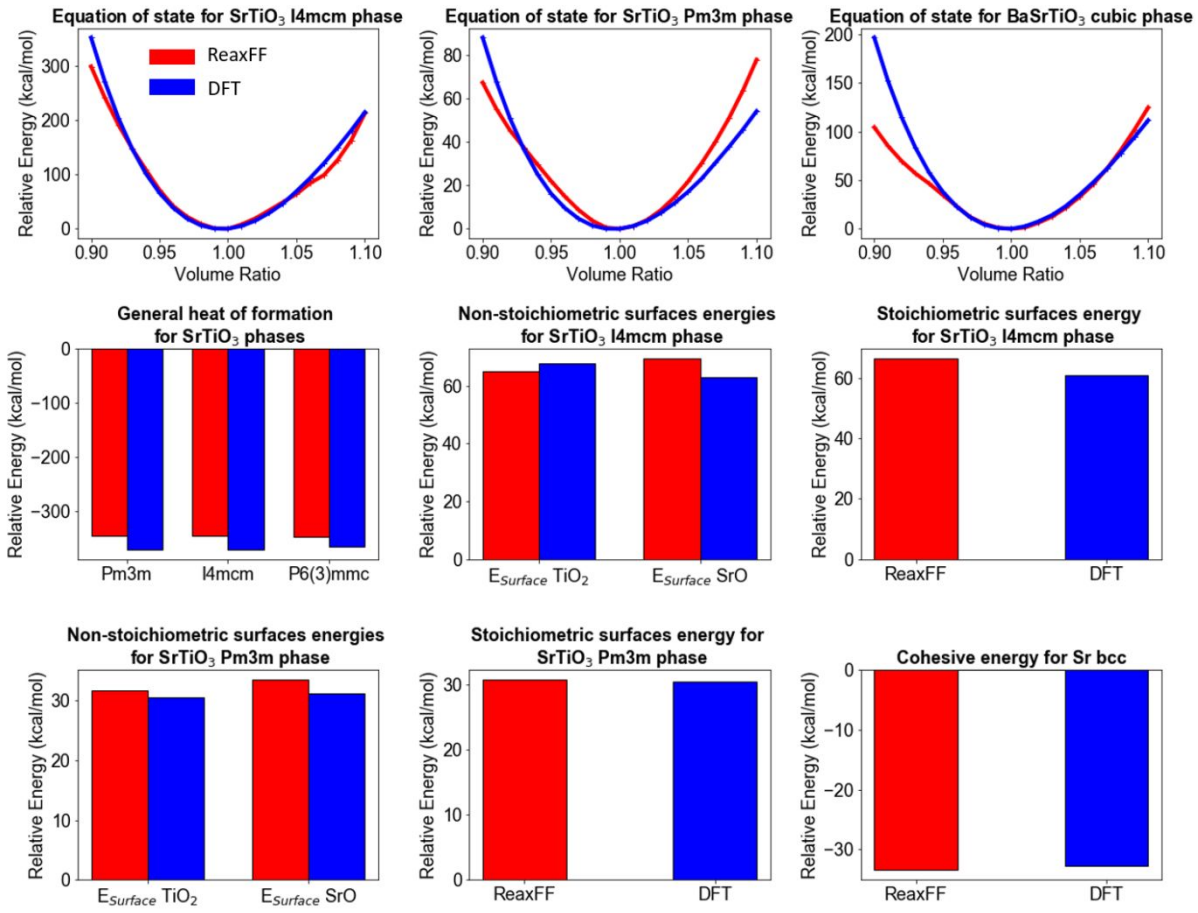

Figure 1. Comparison of ReaxFF and DFT equations of state, heats of formation and stoichiometric/non-stoichiometric surface energies.

Figure 2 illustrates the OV migration path and formation energy in STO. As shown in Figure 2.a, ReaxFF predicts a +79.36 kcal/mol OV formation energy for STO, which is in reasonable agreement with the corresponding DFT value of +137.02 kcal/mol considering that DFT is known to overestimate O_2 stability[17]. More importantly, ReaxFF predicts a 19.5 kcal/mol energy barrier for OV migration in STO (Figure 2.b), which is very close to the energy barrier for OV migration in BTO of 20 kcal/mol[17].

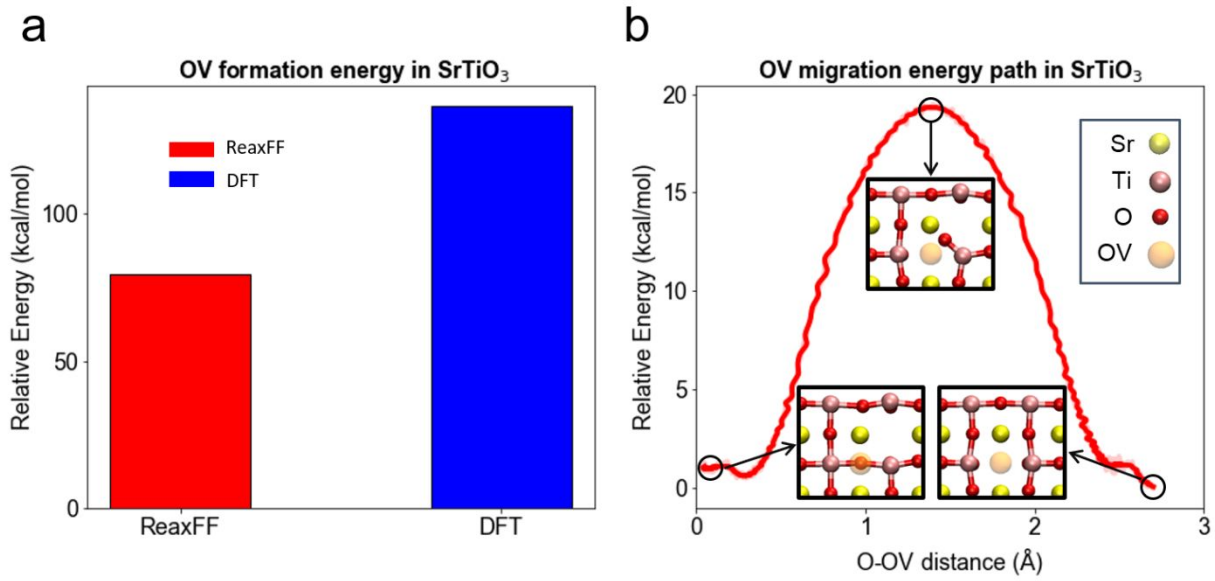

Figure 2. a) Comparison of ReaxFF and DFT for OV formation energy in STO. b) ReaxFF prediction for OV migration energy path in STO.

Figure 3 shows the effects of Sr/Ba ratio on phase transition temperature, lattice parameters and polarization, confirming that ReaxFF can reproduce the tetragonal and cubic phases of BSTO as a function of Sr/Ba ratio. As illustrated in Figure 3.a-e, by increasing the Sr/Ba ratio, the phase transition temperature and the initial polarization of the system both decreased monotonically. A similar observation was reported by Rappe *et al*. based on MD simulations using a BV potential[12]. However, ReaxFF predicts that the cubic structure becomes the dominant phase and initial polarization disappears for Sr/Ba ratios exceeding 15%, while Rappe *et al*. reported the initial polarization in systems with more than 50% Sr. This discrepancy could be associated with rhombohedral to orthorhombic phases that were not incorporated in our BSTO ReaxFF description.

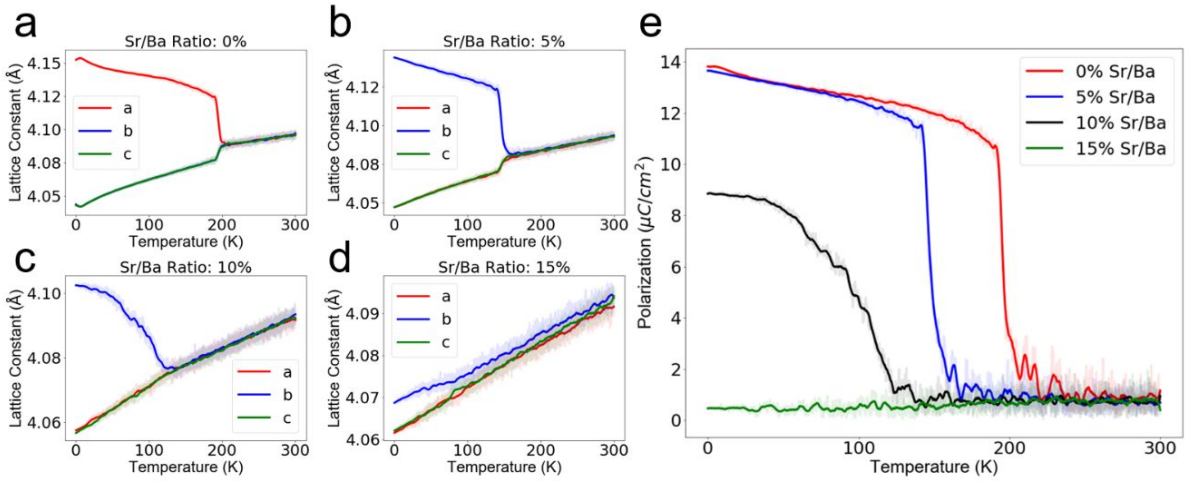

Figure 3. Effects of Sr/Ba ratio on phase transition temperature, lattice parameters and polarization of BSTO. Phase diagrams for a) Sr/Ba=0% (T_c= 210 K), b) Sr/Ba=5% (T_c= 156 K), c) Sr/Ba=10% (T_c= 135 K) and d) Sr/Ba=15% (T_c= 81 K). e) Plot of total polarization vs temperature for different Sr concentrations.

In order to obtain detailed insight into the effects of Sr/Ba ratio on the polarization in the system, the plot of the local polarizations in each unit cell before and after adding Sr to an 8 × 8 × 8 super cell is provided in Figure 4. As Figure 4.a demonstrates, in the absence of Sr, the unit cell polarizations are aligned in [010] direction, characteristic of the tetragonal phase. Increasing the Sr/Ba ratio up to 15% completely distorts and generally reduces the magnitude of local polarizations in unit cells (Figure 4.b), explaining the lack of polarization in Figure 3.e.

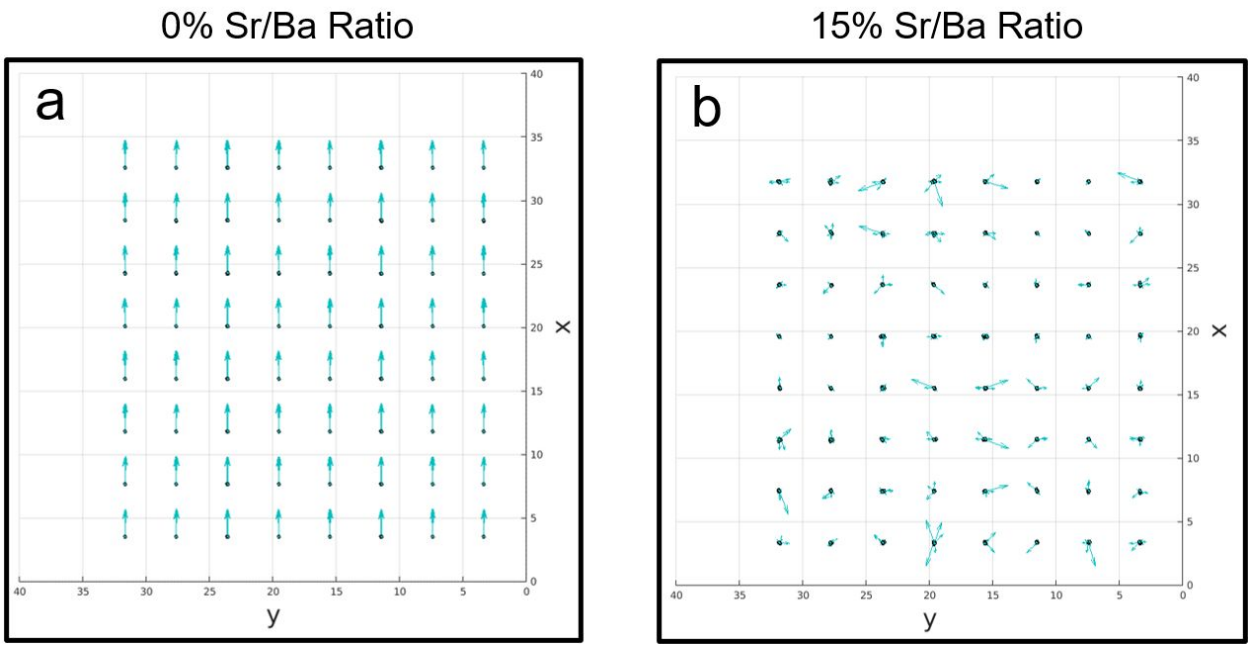

Figure 4. Effects of Sr/Ba ratio on local polarizations in an 8 × 8 × 8 super cell. a) Local polarizations perfectly aligned in x direction in the absence of Sr. b) Local polarizations reduced and oriented in different directions in system with 15% Sr/Ba ratio.

OVs can significantly affect the performance of ferroelectric devices[27-28] by deteriorating the polarization and causing fatigue after frequent polarization switching[27, 29]. However, OVs sometimes may induce favorable properties that do not exist in pure crystals [30-31]. For example, appropriate modulation of OV concentration can elevate STO conductivity to levels difficult to achieve by other techniques[30, 32-33].

We used the new force field to study the effects of different OV concentrations on the polarization and phase transition temperature of BTSO. Figure 5.a-c shows the effects of OVs on lattice constants, phase transition temperature, and initial polarization in BSTO with 5% Sr/Ba ratio. Based on these ReaxFF results, increasing the OV concentration in the system, reduces the initial polarization and the phase transition temperature monotonically. For example, 1.0 % and

2.0 % OV in the system decrease the polarization from its intact value of 13.8 $\mu C/cm^2$ to 2.2 $\mu C/cm^2$ and 1.1 $\mu C/cm^2$, respectively. Similarly, the phase transition temperature decreases from 220 *K* to 118 *K* (1.0 % OV) and 70 *K* (2.0 % OV), in line with reported classical MD and first principles studies [34-36]. The effects of OVs in BSTO systems are more severe than the OV effects in BTO systems. For instance, a 1.0 % OV concentration yields an initial polarization of 11.52 $\mu C/cm^2$ in a BTO system, but only 2.2 $\mu C/cm^2$ in a BSTO system (Sr/Ba ratio: 5%). The OV-induced loss of polarization in ferroelectrics can be attributed to the fact that the unit cell polarization is irreversibly distorted by the presence of OVs[34]. Furthermore, OVs can pin the polarization to a particular direction that causes tail-to-tail polarizations along the *Ti-OV-Ti* pattern as well as polarization suppression[36].

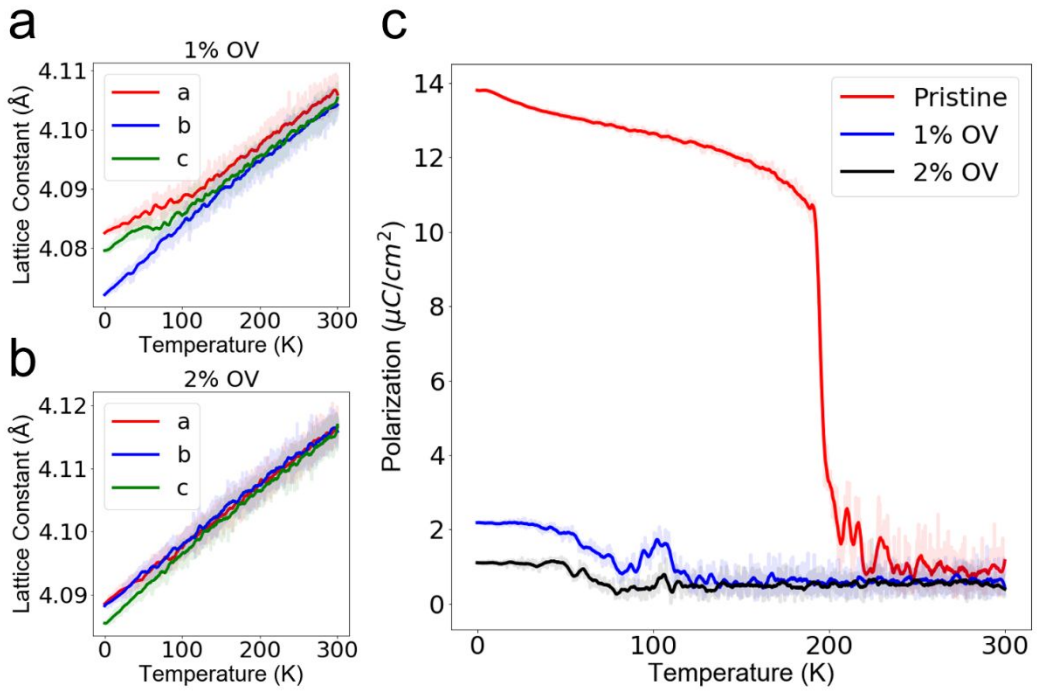

Figure 5. Effects of OV concentration on phase transition temperature, lattice parameters and polarization of BSTO with 5% Sr/Ba ratio. Phase diagram for a) 1% OVs (T_c= 120K) and b) 2%

OVs in the system (T_c= 75K). c) Plot of total polarization vs temperature for different OV concentrations.

Atomistic-level investigation of water adsorption on ferroelectric surfaces is essential for deep understanding of BSTO ferroelectrics properties [37-38]. Accordingly, we further employed our new force field to evaluate the effect of surface chemistry on the polarization of a 14.6 *nm* BSTO slab with TiO_2 [0 0 1] surface terminations. As illustrated in Figure 6, the surfaces are screened due to adsorption of H_2O molecules on the surfaces of the slab. The charge screening induced by adsorption of H_2O molecules on the surfaces leads to an increase in the initial polarization up to 3.7 $\mu C/cm^2$ (compared to 2.6 $\mu C/cm^2$ for the non-hydrated simulation)[39]. This observation is in agreement with previous studies wherein charge screening caused by molecular adsorbates such as hydroxyl and carboxylate were found to reduce the critical size of BTO nanoparticles[40-41]. The molecular adsorbates such as H_2O and OH groups on the surfaces of BSTO compensate the surface polarization charges and decrease the depolarization energy, which is the energy associated with the depolarization field induced by the surface charges caused by the spontaneous polarization, and consequently this leads to an increased polarization of the system[41]. Our findings indicate that the new force field can effectively be utilized to investigate interactions and applications of BSTO compounds in multi-material interfaces.

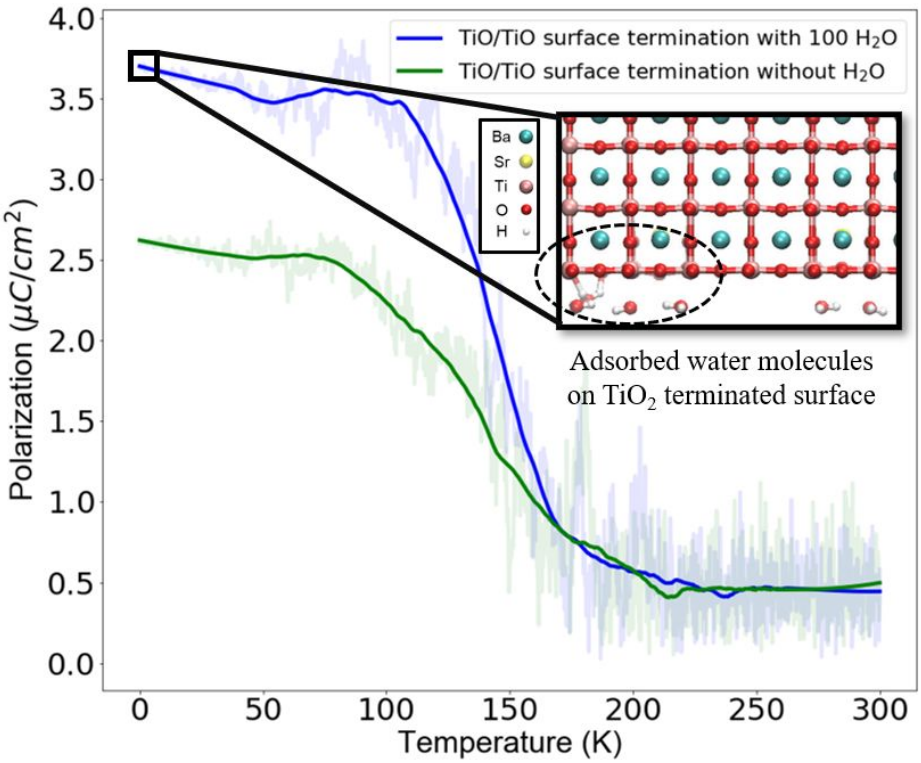

Figure 6. Effects of water interaction with TiO_2 terminated surfaces of a 14.6 *nm* BSTO slab on the polarization. The charge screening induced by adsorption of H_2O molecules on TiO_2 terminated surfaces leads to an increased amount of initial polarization from 2.6 $\mu C/cm^2$ (green line) to 3.7 $\mu C/cm^2$ (blue line).

Conclusion

In this study, we developed a ReaxFF reactive force field verified against DFT data to describe the ferroelectric and non-ferroelectric phases of BSTO. Since ferroelectrics such as BSTO have a remarkable concentration of defects, OVs were also considered in the force field description to improve the realism of the developed force field. Using this force field, a series of MD simulations were carried out to explore the effects of Sr/Ba ratio, OVs and surface chemistry on the ferroelectric properties of BSTO. On the basis of our simulations, increasing the Sr/Ba ratio or adding OVs reduces the polarization and the phase transition temperature of BSTO systems

monotonically. Moreover, we demonstrated that charge screening due to adsorption of H_2O molecules on the TiO_2 terminated surfaces of a BSTO slab leads to increased polarization relative to a BSTO slab with unscreened TiO_2 surfaces. The agreement between the ReaxFF results and available experimental and *ab initio* data shows the strength and the capabilities of the developed ReaxFF reactive force field. Additionally, since the STO substrate is one of the most-used oxide substrates in the epitaxial growth of 2D materials such as transition metal dichalcogenides (TMD), topological insulators, group III-IV metals, the new force field framework is explicitly designed to model the stoichiometric and non-stoichiometric STO surfaces with SrO and TiO_2 terminations. In future studies, we will also pursue the extension of this force field to the substrate interactions of TMD with STO. Our force field only considers the tetragonal and cubic phases, but this limitation does not significantly affect the practical application of the force field since these are the relevant phases for most of the applications of BSTO and these are the main phases related to the working conditions of the electronic devices. EEM indeed has limitations – but it does provide significant transferability with existing ReaxFF force fields, which significantly helps extension of BSTO force field to other materials and interfaces. We will certainly be interested to explore improved charge methods, like ACKS2, and/or include Drude-like electronic degrees of freedom, like in the e-ReaxFF approach, to improve the polarization response[42-43]. In a nutshell, this force field provides an accurate and computationally inexpensive technique to further investigate the role of defects and multi-material interfaces on domain switching and ferroelectric responses that can be very useful for many applications including ferroelectric interfaces in micro electronic devices and for simulations on the material growth on STO support.

Supporting Information

The developed force field as well as the training set are provided free of charge on the PCCP website.

Acknowledgements. We acknowledge funding support from National Science Foundation (NSF) through the Pennsylvania State University 2D Crystal Consortium–Materials Innovation Platform (2DCC-MIP) under NSF cooperative agreement DMR-1539916, from Grant No. AFRL FA9451-16-1-0041 and from AFOSR MURI Contract No. FA9550-19-1-0008.

References

1. Oh, S.; Park, J.-H.; Akedo, J., Dielectric characteristics of barium strontium titanate films prepared by aerosol deposition on a Cu substrate. *IEEE transactions on ultrasonics, ferroelectrics, and frequency control* **2009,** *56* (3), 421-424.
2. Hwang, C. S.; Park, S. O.; Cho, H. J.; Kang, C. S.; Kang, H. K.; Lee, S. I.; Lee, M. Y., Deposition of extremely thin (Ba, Sr) TiO3 thin films for ultra-large-scale integrated dynamic random access memory application. *Applied physics letters* **1995,** *67* (19), 2819-2821.
3. Chen, C.; Feng, H.; Zhang, Z.; Brazdeikis, A.; Huang, Z.; Chu, W.; Chu, C.; Miranda, F.; Van Keuls, F.; Romanofsky, R., Epitaxial ferroelectric Ba 0.5 Sr 0.5 TiO 3 thin films for room-temperature tunable element applications. *Applied physics letters* **1999,** *75* (3), 412-414.
4. Mohammadi, M. R.; Fray, D. J., Sol–gel derived nanocrystalline and mesoporous barium strontium titanate prepared at room temperature. *Particuology* **2011,** *9* (3), 235-242.
5. Joshi, P.; Cole, M., Mg-doped Ba 0.6 Sr 0.4 TiO 3 thin films for tunable microwave applications. *Applied Physics Letters* **2000,** *77* (2), 289-291.
6. Lindner, J.; Weiss, F.; Senateur, J.; Haessler, W.; Köbernik, G.; Oswald, S.; Figueras, A.; Santiso, J., Growth of BaTiO3/SrTiO3 superlattices by injection MOCVD. *Integrated Ferroelectrics* **2000,** *30* (1-4), 53-59.
7. Chen, P.; Xu, W.; Gao, Y.; Warner, J. H.; Castell, M. R., Epitaxial growth of monolayer MoS2 on SrTiO3 single crystal substrates for applications in nanoelectronics. *ACS Applied Nano Materials* **2018,** *1* (12), 6976-6988.
8. Tampo, H.; Asahi, H.; Hiroki, M.; Asami, K.; Gonda, S., Strong photoluminescence emission from GaN on SrTiO3. *physica status solidi (b)* **1999,** *216* (1), 113-116.
9. Zhang, G.; Qin, H.; Chen, J.; He, X.; Lu, L.; Li, Y.; Wu, K., Growth of topological insulator Bi2Se3 thin films on SrTiO3 with large tunability in chemical potential. *Advanced Functional Materials* **2011,** *21* (12), 2351-2355.
10. Van Duin, A. C.; Dasgupta, S.; Lorant, F.; Goddard, W. A., ReaxFF: a reactive force field for hydrocarbons. *The Journal of Physical Chemistry A* **2001,** *105* (41), 9396-9409.
11. Tinte, S.; Stachiotti, M.; Phillpot, S.; Sepliarsky, M.; Wolf, D.; Migoni, R., Ferroelectric properties of BaxSr1− xTiO3 solid solutions obtained by molecular dynamics simulation. *Journal of Physics: Condensed Matter* **2004,** *16* (20), 3495.

12. Wexler, R. B.; Qi, Y.; Rappe, A. M., Sr-induced dipole scatter in Ba x Sr 1− x TiO 3: Insights from a transferable-bond valence-based interatomic potential. *Physical Review B* **2019,** *100* (17), 174109.
13. Noordhoek, M. J.; Krayzman, V.; Chernatynskiy, A.; Phillpot, S. R.; Levin, I., Atomistic structure of (Ba, Sr) TiO3: Comparing molecular-dynamics simulations with structural measurements. *Applied Physics Letters* **2013,** *103* (2), 022909.
14. Qi, Y.; Liu, S.; Grinberg, I.; Rappe, A. M., Atomistic description for temperature-driven phase transitions in BaTiO 3. *Physical Review B* **2016,** *94* (13), 134308.
15. Chenoweth, K.; Van Duin, A. C.; Goddard, W. A., ReaxFF reactive force field for molecular dynamics simulations of hydrocarbon oxidation. *The Journal of Physical Chemistry A* **2008,** *112* (5), 1040-1053.
16. Senftle, T. P.; Hong, S.; Islam, M. M.; Kylasa, S. B.; Zheng, Y.; Shin, Y. K.; Junkermeier, C.; Engel-Herbert, R.; Janik, M. J.; Aktulga, H. M., The ReaxFF reactive force-field: development, applications and future directions. *npj Computational Materials* **2016,** *2* (1), 1-14.
17. Akbarian, D.; Yilmaz, D. E.; Cao, Y.; Ganesh, P.; Dabo, I.; Munro, J.; Van Ginhoven, R.; van Duin, A. C., Understanding the influence of defects and surface chemistry on ferroelectric switching: a ReaxFF investigation of BaTiO 3. *Physical Chemistry Chemical Physics* **2019,** *21* (33), 18240-18249.
18. Mortier, W. J.; Ghosh, S. K.; Shankar, S., Electronegativity-equalization method for the calculation of atomic charges in molecules. *Journal of the American Chemical Society* **1986,** *108* (15), 4315-4320.
19. Van Duin, A. C.; Merinov, B. V.; Han, S. S.; Dorso, C. O.; Goddard Iii, W. A., ReaxFF reactive force field for the Y-doped BaZrO3 proton conductor with applications to diffusion rates for multigranular systems. *The Journal of Physical Chemistry A* **2008,** *112* (45), 11414-11422.
20. Kim, S.-Y.; Kumar, N.; Persson, P.; Sofo, J.; van Duin, A. C.; Kubicki, J. D., Development of a ReaxFF reactive force field for titanium dioxide/water systems. *Langmuir* **2013,** *29* (25), 7838-7846.
21. Kresse, G.; Furthmüller, J., Efficient iterative schemes for ab initio total-energy calculations using a plane-wave basis set. *Physical review B* **1996,** *54* (16), 11169.
22. Blöchl, P. E., Projector augmented-wave method. *Physical review B* **1994,** *50* (24), 17953.
23. Kresse, G.; Joubert, D., From ultrasoft pseudopotentials to the projector augmented-wave method. *Physical review b* **1999,** *59* (3), 1758.
24. Csonka, G. I.; Perdew, J. P.; Ruzsinszky, A.; Philipsen, P. H.; Lebègue, S.; Paier, J.; Vydrov, O. A.; Ángyán, J. G., Assessing the performance of recent density functionals for bulk solids. *Physical Review B* **2009,** *79* (15), 155107.
25. Tian, X.; Wang, T.; Fan, L.; Wang, Y.; Lu, H.; Mu, Y., A DFT based method for calculating the surface energies of asymmetric MoP facets. *Applied Surface Science* **2018,** *427*, 357-362.
26. Wang, G. Z.; Li, C. R.; Cui, J.; Man, Z. Y., Ab initio study of ATiO3 (001) surfaces. *Surface and Interface Analysis: An International Journal devoted to the development and application of techniques for the analysis of surfaces, interfaces and thin films* **2009,** *41* (12-13), 918-923.
27. Cockayne, E.; Burton, B. P., Dipole moment of a Pb-O vacancy pair in PbTiO 3. *Physical Review B* **2004,** *69* (14), 144116.

28. Tselev, A.; Ganesh, P.; Qiao, L.; Siemons, W.; Gai, Z.; Biegalski, M. D.; Baddorf, A. P.; Kalinin, S. V., Oxygen control of atomic structure and physical properties of SrRuO3 surfaces. *ACS nano* **2013,** *7* (5), 4403-4413.
29. Zhang, Y.; Li, J.; Fang, D., Oxygen-vacancy-induced memory effect and large recoverable strain in a barium titanate single crystal. *Physical Review B* **2010,** *82* (6), 064103.
30. Tufte, O.; Chapman, P., Electron mobility in semiconducting strontium titanate. *Physical Review* **1967,** *155* (3), 796.
31. Ren, X., Large electric-field-induced strain in ferroelectric crystals by point-defect-mediated reversible domain switching. *Nature materials* **2004,** *3* (2), 91.
32. Lopez-Bezanilla, A.; Ganesh, P.; Littlewood, P. B., Magnetism and metal-insulator transition in oxygen-deficient SrTiO 3. *Physical Review B* **2015,** *92* (11), 115112.
33. Zhuang, H. L.; Ganesh, P.; Cooper, V. R.; Xu, H.; Kent, P., Understanding the interactions between oxygen vacancies at SrTiO 3 (001) surfaces. *Physical Review B* **2014,** *90* (6), 064106.
34. Wang, J.; Shen, Y.; Song, F.; Ke, F.; Bai, Y.; Lu, C., Effects of oxygen vacancies on polarization stability of barium titanate. *Science China Physics, Mechanics & Astronomy* **2016,** *59* (3).
35. Chen, Y.; Liu, B.; Ma, Y.; Zhou, Y., Modification of a shell model for the study of the radiation effects in BaTiO3. *Nuclear Instruments and Methods in Physics Research Section B: Beam Interactions with Materials and Atoms* **2009,** *267* (18), 3090-3093.
36. Li, M.; Li, J.; Chen, L.-Q.; Gu, B.-L.; Duan, W., Effects of strain and oxygen vacancies on the ferroelectric and antiferrodistortive distortions in PbTiO 3/SrTiO 3 superlattice. *Physical Review B* **2015,** *92* (11), 115435.
37. Li, X.; Wang, B.; Zhang, T.-Y.; Su, Y., Water adsorption and dissociation on BaTiO3 single-crystal surfaces. *The Journal of Physical Chemistry C* **2014,** *118* (29), 15910-15918.
38. He, D.; Qiao, L.; Khodayari, M.; Volinsky, A. A., Electric field and humidity effects on adsorbed water behavior on BaTiO3 ferroelectric domains studied by scanning probe microscopy. *Journal of Applied Physics* **2014,** *116* (8), 084105.
39. Li, X.; Bai, Y.; Wang, B.; Su, Y., Water adsorption induced in-plane domain switching on BaTiO3 surface. *Journal of Applied Physics* **2015,** *118* (9), 094104.
40. Spanier, J. E.; Kolpak, A. M.; Urban, J. J.; Grinberg, I.; Ouyang, L.; Yun, W. S.; Rappe, A. M.; Park, H., Ferroelectric phase transition in individual single-crystalline BaTiO3 nanowires. *Nano letters* **2006,** *6* (4), 735-739.
41. Yasui, K.; Kato, K., Influence of adsorbate-induced charge screening, depolarization factor, mobile carrier concentration, and defect-induced microstrain on the size effect of a BaTiO3 nanoparticle. *The Journal of Physical Chemistry C* **2013,** *117* (38), 19632-19644.
42. Verstraelen, T.; Ayers, P.; Van Speybroeck, V.; Waroquier, M., ACKS2: Atom-condensed Kohn-Sham DFT approximated to second order. *The Journal of chemical physics* **2013,** *138* (7), 074108.
43. Islam, M. M.; Kolesov, G.; Verstraelen, T.; Kaxiras, E.; Van Duin, A. C., eReaxFF: a pseudoclassical treatment of explicit electrons within reactive force field simulations. *Journal of chemical theory and computation* **2016,** *12* (8), 3463-3472.